

SCWR CHEMISTRY ISSUES: HYDROTHERMAL STABILITY OF HYDRAZINE

Andriy Plugatyr, Tina Hayward and Igor M. Svishchev
Trent University, Ontario, Canada

Abstract

Hydrazine is one of the potential candidates for chemistry control for both in-core and out-of-core components of a SCWR. At present, systematic experimental data on hydrazine chemistry is mainly limited to sub-critical water conditions. Supercritical water flow-through test facility for the study of hydrothermal processes is described. The decomposition of hydrazine in aqueous solution is examined along the 25 MPa isobar. The obtained first-order rate constant for the thermal decomposition of hydrazine increases from $3.73 \times 10^{-4} \text{ s}^{-1}$ at 473 K to about 0.31 s^{-1} at 725 K.

1. Introduction

The supercritical water-cooled reactor (SCWR) concept is a direct cycle operating at the pressure of 25 MPa with core inlet and outlet temperatures of about 550 K and up to 900 K, respectively [1]. At present, the lack of knowledge of supercritical water (SCW) chemistry under irradiation conditions is one of the main obstacles in the development of the SCWR [2]. A thorough understanding of factors controlling corrosion and corrosion product transport is needed for the selection of materials and specifications of key water chemistry parameters (pH, dissolved oxygen/hydrogen concentrations, other additives, etc.) to ensure safe and reliable long-term operation of the supercritical water-cooled reactor.

The current chemistry control strategy in pressurized water reactors (PWR) involves operation under alkaline conditions ($\text{pH}_{300^\circ\text{C}} > 6.9$), through the addition of lithium hydroxide, to minimize corrosion and corrosion product transport [3]. The in-core generation of oxidizing species, such as H_2O_2 , $\cdot\text{OH}$, and O_2 due to the radiolytic breakdown of water is suppressed by the addition of hydrogen gas to the coolant at a concentration of $25\text{-}50 \text{ cm}^3\cdot\text{kg}^{-1}$ (also known as Hydrogen Water Chemistry (HWC)). It is not clear whether the PWR water chemistry specifications will provide adequate chemistry control above the critical point of water. For instance, pH control in low density supercritical water may prove to be difficult (if possible at all) due to the low dielectric constant of the medium. The efficiency of HWC in reducing concentrations of radiolytic products is also uncertain, due to the decrease in the critical reaction rate constant between the $\cdot\text{OH}$ and hydrogen, recently reported for water above 573 K [4].

Among the water chemistries employed at once-through supercritical fossil-fired SCW power plants [5] are Oxygenated Water Treatment (OT) and All Volatile Treatment (AVT). In OT, oxygen is added to the demineralized ($< 0.2 \mu\text{S}\cdot\text{cm}^{-1}$) alkaline ($\text{pH}_{25^\circ\text{C}} = 8.0\text{-}8.5$ (ammonia)) feed water at a concentration of 30-150 ppb. In contrast, the AVT relies on complete removal of oxygen ($< 5 \text{ ppb}$) using hydrazine as an oxygen scavenger with the pH_{25} adjusted to about 9 using ammonia.

Hydrazine is, arguably, one of the potential candidates for chemistry control for both in-core and out-of-core components of the SCWR. Above room temperature, hydrazine decomposes primarily into

ammonia and nitrogen, both acceptable products for the nuclear plant chemistry. At present, available systematic experimental data on hydrazine kinetics is largely limited to sub-critical water conditions. Thermal decomposition of pure hydrazine up to 523 K and about 3 MPa has been examined by Lucien [6]. Buelow *et al.* [7] and Masten *et al.* [8] have examined the decomposition of hydrazine in sub- and supercritical water along the 360 atm isobar by using *in situ* Raman spectroscopy. Several studies have focused on the oxidation of hydrazine [9, 10]. Radiolysis of aqueous hydrazine solutions has been examined up to 473 K by Buxton and Stuart [11-13]. Utilization of hydrazine hydrate for *in situ* hydrogen generation to suppress water radiolysis has been reported for VVER (water-cooled, water-moderated) reactors [14]. The thermal and radiation characteristics of hydrazine in the primary loop of VVER reactors are discussed by Arkhipov *et al.* [9]. Investigation of the reactivity of hydrazine near and above the critical point of water for its potential use for in-core chemistry control of the SCWR is clearly warranted.

The first goal of this study was to examine the hydrodynamics of a pressurized fluid flow at sub- and supercritical water conditions by conducting residence time distribution measurements (RTD). It is worth mentioning that the results of our recent RTD study demonstrate that hydrothermal reactors may exhibit non-ideal hydrodynamic behavior [15]. Consequently, experimental determination of the mean residence time of the fluid in the “hot zone” of the flow-through system is crucial for obtaining reliable kinetics data particularly at supercritical water conditions. The second, and the main, goal of this study was to examine the thermal decomposition of hydrazine hydrate in a flow under the operating conditions relevant to the SCWR.

2. Experimental Apparatus and Procedures

2.1 Experimental apparatus

The employed bench-top flow-through supercritical water test facility (SCW TF) is shown in Fig. 1 (a-c). The pressure in the system was maintained by an HPLC pump (Waters® 590). The system is equipped with a six-port two-position electrically actuated sample injection valve (Valco®) which is used to carry out flow injection experiments. The reactor (in Fig. 1c) was constructed of a stainless steel 316 (SS316) tube ($ID = 2.1\text{ mm}$, $L = 200\text{ mm}$). Two SS316 frits with $2\text{ }\mu\text{m}$ porosity were installed at the inlet and outlet of the reactor in order to minimize back-mixing of the fluid. The fluid was preheated to the operating temperature by passing it through a coiled capillary ($ID = 0.75\text{ mm}$, $L = 3\text{ m}$) before entering the reactor. The preheater and the reactor were placed in a custom made sand bath which sits inside a muffle furnace (Isotemp® 650 Series, Fisher Scientific®). The temperature of the furnace was maintained by the built-in PID controller equipped with a K-thermocouple. A custom built heat exchanger ($L = 2.5\text{ m}$), coupled to a cold plate (TE Technology®, Inc.), was used to cool down the effluent to ambient temperature. The temperature of the heat exchanger was maintained at $25\text{ }^\circ\text{C}$ by a temperature controller (TC-24-25, TE Technology®). The pressure in the system was controlled by an adjustable back pressure regulator (P-880, Upchurch®). Both temperature and pressure in the system were monitored using a data logger (PrTC-210, Omega®). Cooled and depressurized effluent was passed through a 10 mm optical path stainless steel flow cell (FIA-Z-SMA, FIA Inc.®). On-line spectroscopic measurements were performed using an UV-Vis spectrometer (USB-2000, Ocean Optics®). Oxygen levels were monitored on-line using NeoFox system (Ocean Optics®) equipped with FOXY-R oxygen sensor. All parts of the flow-through apparatus were constructed of stainless steel

SS316 tubing (*OD* = 1.6 mm, *ID* = 0.75 mm) and connected using SS316 zero dead volume unions (Valco).

2.2 Residence time distribution measurements

The RTD experiments were carried out at 25 MPa from 298 to 773 K with volumetric flow rates at the pump ranging from 0.1 to 1.0 ml·min⁻¹. Above 373K experiments were performed at 100 K intervals. Due to its high thermal stability, phenol was used as a tracer compound. Tracer phenol solution (100 ppm) was prepared from 1000 ppm phenol standard (LabChem Inc.) using demineralized (MilliQ) water. Both the carrier water and the tracer phenol solution were deoxygenated by helium sparging. Prior to injection, the system was allowed to stabilize at the set operating conditions for about two hours. Subsequently, 250 µl of the tracer solution was injected into the flow system. The injection event was synchronized with the time acquisition of the UV-Vis spectra. Phenol in the effluent was detected spectrophotometrically at a wavelength of 270 nm.

At each state point, several RTD measurements were performed. The experimental RTD curves were characterized by calculating the first two moments of the distribution. The first moment, which corresponds to the mean residence time of the fluid in the vessel, τ , is given by:

$$\tau = \int t \cdot C(t) dt , \quad (1)$$

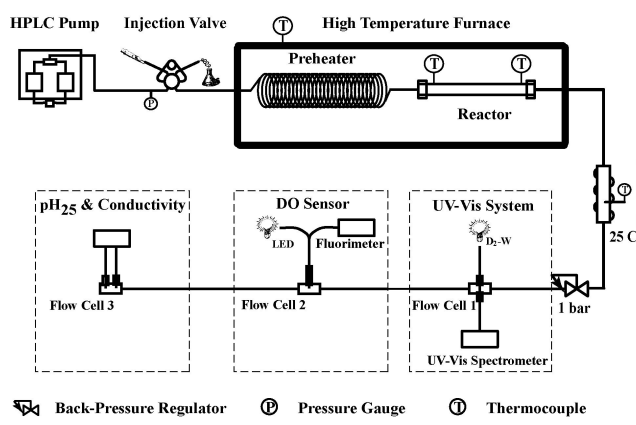
where $C(t)$ is the normalized exit concentration of the tracer (i.e. $\int C(t) dt = 1$) at time t .

2.3 Thermal decomposition of hydrazine

Thermal decomposition of hydrazine in aqueous solution was studied at 25 MPa from 473 to 723 K. The experiments were performed with feed hydrazine concentrations ranging from 10 to 1000 ppm. The working hydrazine solutions were prepared in demineralized deoxygenated water using pure hydrazine hydrate (Fluka, 98%+). Residual oxygen concentrations in the feed solution were determined to be below the detection limit of the oxygen sensor (< 20 ppb). Prior to each measurement the flow system was allowed to equilibrate for at least two hours. The feed and effluent concentrations of hydrazine were determined spectrophotometrically according to the method described by Amlathe and Gupta [16]. A 100 ppm hydrazine hydrochloride standard (Ricca Chemical) was used to prepare standard solutions. The average concentration of hydrazine in the feed and effluent was calculated from three and five grab samples, respectively. At least three replicate experiments were performed at each state point examined.



(a)



(b)



(c)

Figure 1 (a) Photograph and (b) schematics of the flow-through SCW test facility. (c) Photograph of the tubular reactor and preheater.

3. Experimental Apparatus and Procedures

3.1 Residence time distribution measurements

The results of the RTD measurements indicate that at 25 MPa, the constructed flow system exhibits nearly ideal hydrodynamic behavior over the examined temperature and flow rate ranges. The RTD curves show excellent reproducibility and are virtually Gaussian in shape (small extent of axial dispersion). Overall, the relative error of the mean residence time does not exceed 2.85%, with average value being less than 1%. Average relative fluctuations in temperature and pressure were below 0.55 % in all experiments.

In this study, we have used the experimentally determined mean residence times along with the corresponding volumetric flow rates to calculate the effective volume of the flow through system as a function of operating density. The total effective volume of the system, $V_{Tot}(T, p)$, was obtained according to Eq. 2:

$$V_{Tot}(T, p) = \bar{\tau}(T, p, F) \cdot F, \quad (2)$$

where $\bar{\tau}(T, p, F)$ is the experimental mean residence time of the fluid at given operating temperature, T , pressure, p , and volumetric flow rate at the pump, F . The density of the fluid in the “hot zone” was calculated from experimental temperature and pressure measurements by using the GERG-2004 equation-of-state for water [17]. The results reveal that the total effective volume of the flow-through system, $V_{Tot}(T, p)$, is a linear function of the operating density, $\rho(T, p)$, and can be mathematically described as:

$$V_{Tot}(T, p) = V_{CRZ} + V_{HRZ} \frac{\rho(T, p)}{\rho(T^*, p)}, \quad (3)$$

where V_{CRZ} and V_{HRZ} are volumes of “cold” and “hot” zones of the flow-through system, respectively, and T^* is ambient temperature. Essentially, V_{CRZ} corresponds to the volume of the fluid in the flow-through system that is not affected by the change in density upon heating at fixed pressure, whereas V_{HRZ} represents the volume of the “hot” system’s zone, which includes the reactor and some portion of the preheater/heat exchanger tubing. The observed linear variation of the V_{Tot} with density suggests that at examined flow rates the heating/cooling of the fluid is very rapid and can be approximated by a step function. This assumption is supported by the computational fluid dynamics (CFD) calculations performed by Masten *et al.*[8] for a similar reactor configuration ($ID = 1.57$ mm and $L = 51$ mm). Their CFD results indicate that the heat-up time to 673K with the flow rate up to 3 ml/min is less than 3 s. At these heat-up times, the uncertainty in the estimation of the residence times is very small.

3.2 Thermal decomposition of hydrazine hydrate

The rate of the thermal decomposition of hydrazine in the flow-through system was determined by measuring the initial (feed) and final (effluent) concentrations of hydrazine. The reaction times were controlled by the volumetric flow rate at the pump. The mean residence time of the fluid in the “hot zone” of the flow system was calculated by using a plug flow model:

$$\bar{\tau}(T, p, F) = \frac{V_{HRZ} \cdot \rho(T, p)}{F \cdot \rho(T^*, p)}, \quad (4)$$

where V_{HRZ} is the volume of “hot zone”, $\rho(T, p)$ is the operating density, F is the volumetric flow rate at the pump and $\rho(T^*, p)$ is the density of the fluid at ambient temperature, T^* . As in the RTD study, the density of the fluid in the “hot zone” was calculated from the GERG-2004 formulation [17]. The experimental results for the thermal decomposition of hydrazine hydrate in aqueous solution are plotted in Fig. 2. As expected, the effective first-order rate constant increases along the 25 MPa isobar from $3.73 \times 10^{-4} \text{ s}^{-1}$ at 473 K to about 0.31 s^{-1} at 725 K. The average mean relative error for the measured rate constants was determined to be below 7%. Rapid decrease in water density near and above the critical point of water significantly impedes the range of residence times that can be attained over the employed flow rates. The values obtained above 623 K are in somewhat higher uncertainty due to short residence times. Above 723 K the thermal decomposition rate becomes too fast to be accurately determined by *ex situ* techniques.

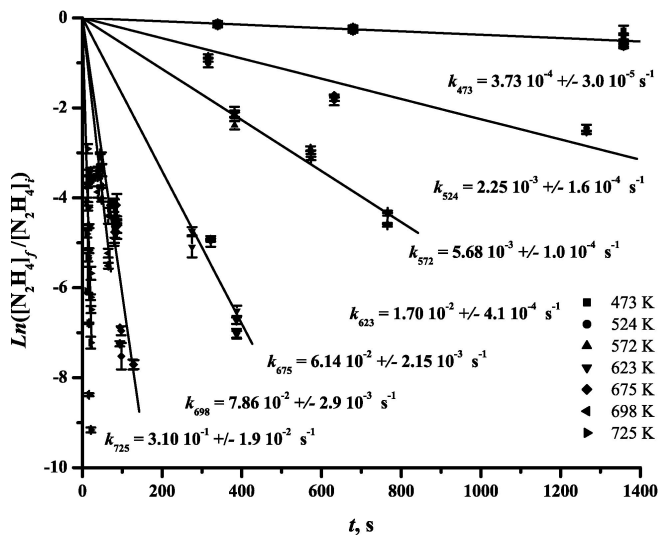


Figure 2 Variation of $\ln([\text{N}_2\text{H}_4]_f/[\text{N}_2\text{H}_4]_i)$ vs. residence time. Error bars represent 95% confidence level. Fitted rate constants are also shown.

The obtained kinetics data is in reasonable agreement with the available literature values. The overall decomposition rate constant of hydrazine in the primary loop of a VVER reactor ($T \approx 573 \text{ K}$, $p \approx 15 \text{ MPa}$), estimated from plant mass-balance considerations, was calculated to be approximately $1.5 \times 10^{-2} \text{ s}^{-1}$ [9]. Please, note that the gross decomposition rate of hydrazine reported by Arkhipov *et al.* includes radiolytic, oxidation and surface reaction pathways. Nevertheless, the reported value of $1.5 \times 10^{-2} \text{ s}^{-1}$ is only about 2.5 times larger than our result of $5.68 \times 10^{-3} \text{ s}^{-1}$ obtained at 573 K and 25 MPa. Masten *et al.* [8] have measured the rate of the decomposition of hydrazine at sub- and supercritical water conditions *in situ* by using Raman spectroscopy. They have reported a value of approximately 0.32 s^{-1} obtained at 673 K and 360 atm, which is somewhat higher than our result of $6.15 \times 10^{-2} \text{ s}^{-1}$ at 673 K and 25 MPa, but compares well with the value of 0.31 s^{-1} obtained in this study at 725 K and 25 MPa. Analysis of obtained kinetics data suggests that over the examined temperature range the decomposition of hydrazine follows Arrhenius behavior with an apparent activation energy of 70.24 kJ/mol. This observation is in accord with earlier *in situ* Raman studies by Buelow *et al.* [7] and Masten

et al. [8] who reported no anomalous change in the rate constant for the decomposition of hydrazine upon transition into the supercritical region. Buelow *et al.* derived a rate expression valid from 280 to 430 °C: $k(s^{-1}, 360 \text{ atm}) = 5.2 \times 10^8 \exp(-14220/T)$. The discrepancy in the reaction rates obtained in this study with the result reported by Buelow *et al.* [7] (see Fig. 3) may be attributed to differences in surface catalyzed decomposition of hydrazine on reactor walls. Previous reports [5] have indicated that the decomposition of hydrazine can be catalyzed by various metals, such as nickel, iron, and copper.

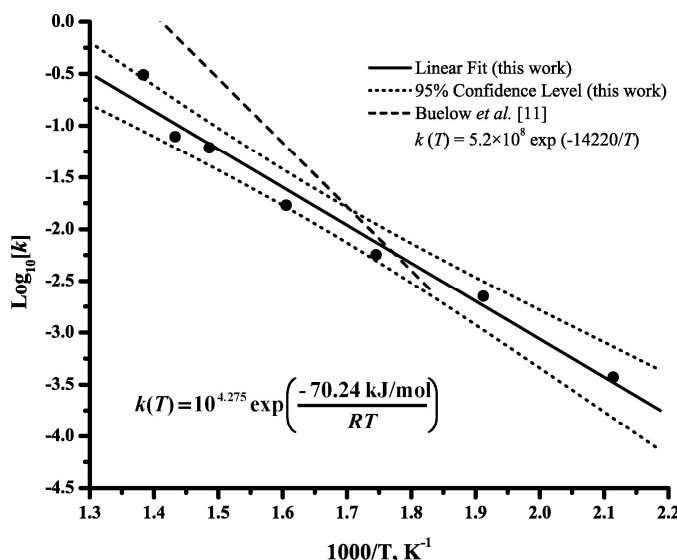


Figure 3 Arrhenius plot for the decomposition of hydrazine in aqueous solution at 25 MPa.

We may also add that for the thermal decomposition of hydrazine the transition from ionic to free radical chemistry [18] can occur at low density supercritical conditions where dielectric constant approaches that of gas phase. At present, the results for the thermal decomposition of hydrazine seem to indicate that the crossover to gas phase chemistry does not occur up to 725 K ($\sim 0.1 \text{ g/cm}^3$, 25 MPa). Further studies of the effect of fluid density (solvent effects) on the reaction rates at near and above the critical point of water are necessary to provide fundamental understanding of the reaction kinetics at sub- and supercritical water conditions.

5. Conclusion

The supercritical water flow-through test facility for the study of hydrothermal fluids has been described. The hydrodynamics of the employed reactor configuration was examined from ambient to supercritical water conditions by conducting RTD measurements. The RTD results indicate that at 25 MPa, the system exhibits plug flow behavior with small extents of dispersion over the examined temperature and flow rate ranges. The experimental data obtained from the RTD measurements was used to determine the volume of the “hot zone” for the flow-through system.

The decomposition of hydrazine in aqueous solution was investigated from 473 to 725 K with pressure fixed at 25 MPa. The obtained first-order rate constant increases from $3.73 \times 10^{-4} \text{ s}^{-1}$ at 473 K to about 0.31 s^{-1} at 725 K and follows Arrhenius behavior with effective pre-exponential factor and activation energy being $10^{4.275} \text{ s}^{-1}$ and 70.24 kJ/mol, respectively.

6. Acknowledgements

This study has been conducted within the framework of the R&D activities of the Canadian National Program on Generation IV Energy Technologies. The authors are grateful for the financial support of the Natural Sciences and Engineering Research Council of Canada (NSERC), Natural Resources of Canada (NRCan) and Atomic Energy of Canada Limited (AECL).

7. References

- [1] C.K. Chow and H.F. Khatabil, Conceptual Fuel Channel Designs for CANDU-SCWR. *Journal of Nuclear Engineering and Technology* 40 (2007) 139-146.
- [2] D. Guzonas, SCWR Materials and Chemistry Status of Ongoing Research, *Proceedings of the GIF Symposium*, September 2009.
- [3] Technical Report, Plant-Specific Optimization of LWR Water Chemistry, EPRI, TR-107329, 1997.
- [4] T.W. Marin, C.D. Jonah and D.M. Bartels, Reaction of ·OH radicals with H₂ in sub-critical water, *Chemical Physics Letters* 371 (2003) 144-149.
- [5] Technical Report, GEN IV Nuclear Energy Systems, Oak Ridge National Laboratory, ORNL/TM-2003/244/R2, December 2005.
- [6] H.W. Lucien, Thermal Decomposition of Hydrazine, *Journal of Chemical and Engineering Data* 6 (1961) 584.
- [7] S. J. Buelow *et al.*, Technical Report, Destruction of Energetic Materials in Supercritical Water, Air Force Research Laboratory, Technical Report, AFRL-ML-TY-TR-2002-4522, June 2002.
- [8] D. A. Masten, B. R. Foy, D. M. Harradine and R. B. Dyer, *In situ* Raman spectroscopy of reactions in supercritical water, *Journal of Physical Chemistry* 97 (1993), 8557-8559.
- [9] O.P. Arkhipov, V.L. Bugaenko, S.A. Kabakchi and V.I. Pashevich, Thermal and radiation characteristics of hydrazine in the primary loop of nuclear power plants with water-cooled, water-moderated reactors, *Atomic Energy* 82 (1997) 92 - 98.
- [10] K. Ishida, Y. Wada, M. Tachibana, M. Aizawa, M. Motomasa and E. Kadoi, Hydrazine and Hydrogen Co-injection to Mitigate Stress Corrosion Cracking of Structural Materials in Boiling Water Reactors, (I) Temperature Dependence of Hydrazine Reactions, *Journal of Nuclear Science and Technology* 43 (2006), 65-76.
- [11] G.V. Buxton and C.R. Stuart, Radiation chemistry of aqueous solutions of hydrazine at elevated temperatures. Part 1. Oxygen-free solutions, *Journal of Chemical Society, Faraday Transactions* 92 (1996) 1519-1525.
- [12] G.V. Buxton and C.R. Stuart, Radiation chemistry of aqueous solutions of hydrazine at elevated temperatures Part 2. Solutions containing oxygen, *Journal of Chemical Society, Faraday Transactions* 93 (1997) 1535-1538.

- [13] G.V. Buxton and D.A. Lynch, Radiation chemistry of aqueous solutions of hydrazine. Part 3. The chain reaction in oxygenated solutions irradiated with ^{60}Co γ -rays, Physical Chemistry Chemical Physics 1 (1999), 3293-3296.
- [14] Technical Report, Review of VVER Primary Water Chemistry and the Potential for its Use in PWRs, EPRI 1003382, September 2002; Technical Report, Coolant technology of water cooled reactors, IAEA, IAEA-TECDOC-667, September 1992.
- [15] A. Plugatyr and I.M. Svishchev, Residence time distribution measurements and flow modeling in a supercritical water oxidation reactor: Application of transfer function concept. Journal of Supercritical Fluids 44 (2008) 31-39.
- [16] S. Amlathe, and V.K. Gupta, Spectrophotometric determination of trace amounts of hydrazine in polluted water, Analyst 113 (1988) 1481-1483.
- [17] O. Kunz, R. Klimeck, W. Wagner and M. Jaeschke, The GERG-2004 wide-range equation of state for natural gases and other mixtures, Fortschr.-Ber. VDI, Dusseldorf, 2007.
- [18] J. A. Kerr, R. C. Sekhar and A. F. Trotman-Dickenson, The Pyrolyses of Hydrazines and Benzylamines. C-C and N-N Bond Dissociation Energies, Journal of Chemical Society B (1963) 3217-3225